Available online at www.sciencedirect.com

ScienceDirect

Geochimica et Cosmochimica Acta 224 (2018) 249–261

Geochimica et Cosmochimica Acta

www.elsevier.com/locate/gca

Distributions of geohopanoids in peat: Implications for the use of hopanoid-based proxies in natural archives

Gordon N. Inglis [a,b,*], B. David A. Naafs [a,b], Yanhong Zheng [c], Erin L. McClymont [d], Richard P. Evershed [a,b], Richard D. Pancost [a,b], the 'T-GRES Peat Database collaborators'

[a] *Organic Geochemistry Unit, School of Chemistry, University of Bristol, Cantock's Close, Bristol BS8 1TS, UK*
[b] *Cabot Institute, University of Bristol, Bristol, UK*
[c] *State Key Laboratory of Continental Dynamics, Department of Geology, Northwest University, Xi'an, PR China*
[d] *Department of Geography, Durham University, Durham, UK*

Received 26 July 2017; accepted in revised form 20 December 2017; available online 9 January 2018

Abstract

Hopanoids are pentacyclic triterpenoids produced by a wide range of bacteria. Within modern settings, hopanoids mostly occur in the biological 17β,21β(H) configuration. However, in some modern peatlands, the C_{31} hopane is present as the 'thermally-mature' 17α,21β(H) stereoisomer. This has traditionally been ascribed to isomerisation at the C-17 position catalysed by the acidic environment. However, recent work has argued that temperature and/or hydrology also exert a control upon hopane isomerisation. Such findings complicate the application of geohopanoids as palaeoenvironmental proxies. However, due to the small number of peats that have been studied, as well as the lack of peatland diversity sampled, the environmental controls regulating geohopanoid isomerisation remain poorly constrained. Here, we undertake a global approach to investigate the occurrence, distribution and diagenesis of geohopanoids within peat, combining previously published and newly generated data (n = 395) from peatlands with a wide temperature (−1 to 27 °C) and pH (3–8) range. Our results indicate that peats are characterised by a wide range of geohopanoids. However, the C_{31} hopane and C_{32} hopanoic acid (and occasionally the C_{32} hopanol) typically dominate. C_{32} hopanoic acids occur as αβ- and ββ-stereoisomers, with the ββ-isomer typically dominating. In contrast, C_{31} hopanes occur predominantly as the αβ-stereoisomer. These two observations collectively suggest that isomerisation is not inherited from an original biological precursor (i.e. biohopanoids). Using geohopanoid ββ/(αβ + ββ) indices, we demonstrate that the abundance of αβ-hopanoids is strongly influenced by the acidic environment, and we observe a significant positive correlation between C_{31} hopane isomerisation and pH ($n = 94$, $r^2 = 0.64$, $p < 0.001$). Crucially, there is no correlation between C_{31} hopane isomerisation and temperature. We therefore conclude that within peats, αβ-hopanoids are acid-catalysed diagenetic products and their occurrence at shallow depths indicates that this isomerisation is rapid. This shows that geohopanoid ββ/(αβ + ββ) indices can be used to reconstruct pH within modern and ancient peat-forming environments. However, we only recommend using ββ/(αβ + ββ) indices to interrogate large amplitude (>1 pH unit) and longer-term (>1 kyr) variation. Overall, our findings demonstrate the potential of geohopanoids to provide unique new insights into understanding depositional environments and interpreting terrestrial organic matter sources in the geological record.
© 2018 The Authors. Published by Elsevier Ltd. This is an open access article under the CC BY-NC-ND license (http://creativecommons.org/licenses/by-nc-nd/4.0/).

Keywords: Bacteria; Hopanoids; Peat; Lignite; Diagenesis; Isomerisation

* Corresponding author at: Organic Geochemistry Unit, School of Chemistry, University of Bristol, Cantock's Close, Bristol BS8 1TS, UK.
E-mail address: gordon.inglis@bristol.ac.uk (G.N. Inglis).

https://doi.org/10.1016/j.gca.2017.12.029
0016-7037/© 2018 The Authors. Published by Elsevier Ltd.
This is an open access article under the CC BY-NC-ND license (http://creativecommons.org/licenses/by-nc-nd/4.0/).

1. INTRODUCTION

Biohopanoids are pentacyclic triterpenoids produced by a wide range of bacteria (Pearson et al., 2007; Rohmer et al., 1984) and appear to perform a regulating and rigidifying function similar to sterols in eukaryotes (Kannenberg and Poralla, 1999; Sáenz et al., 2015). These compounds can be subdivided into two groups: simple hopanoids with a C_{30} ring system (e.g. diploptene/diplopterol) and complex hopanoids with an additional polyfunctionalised side chain (i.e. bacteriohopanepolyols (BHPs)). The latter can be unique markers for specific bacteria (Talbot and Farrimond, 2007) or certain environmental conditions (Bradley et al., 2010) and have been used to profile the bacterial community in terrestrial settings (Höfle et al., 2015; Talbot et al., 2016b). However, due to their polyfunctionalised side chain, BHPs are typically only preserved over relatively recent timescales (e.g. <5 million years; Ma) (Handley et al., 2010; Schefuß et al., 2016; Talbot et al., 2014; Talbot et al., 2016b; Spencer-Jones et al., 2017) and their occurrence in much older sediments (e.g. the Paleocene-Eocene Thermal Maximum; 56 Ma) remains ambiguous (Talbot et al., 2016a).

Instead, reconstructions of the ancient bacterial community are more commonly based upon the abundance (Pancost et al., 2003), distribution (Birgel et al., 2006) and/or stable carbon isotopic composition (Inglis et al., 2015; Pancost et al., 2007) of their degradation products (i.e. geohopanoids). In sediments, with increasing diagenesis, geohopanoids undergo stereochemical transformations and the biologically-derived 17β,21β(H)-hopanoid is transformed into the more thermally stable 17β,21α(H) and 17α,21β(H)-stereoisomers (Mackenzie et al., 1980; Peters and Moldowan, 1991). With increasing maturation, extended hopanoids (>C_{30}) also undergo isomerisation at the C-22 position. Such changes have been widely used to reconstruct the thermal history of sediments (Seifert and Moldowan, 1980; Peters and Moldowan, 1991; Farrimond et al., 1998; Mackenzie et al., 1980), where decreasing ββ/(αβ + ββ) indices and increasing 22S/(22R + 22S) values indicate increasing thermal maturity.

However, whilst geohopanoids in modern sediments typically occur in the biological 17β,21β(H) configuration, in some modern peatlands the 'thermally mature' C_{31} 17α,21β(H)-homohopane (C_{31} αβ hopane, hereafter) dominates over the biological 17β,21β(H) isomer (Dehmer, 1993; Pancost et al., 2003; Quirk et al., 1984; Rohmer et al., 1984; Zhang et al., 2009). The predominance of the C_{31} αβ hopane in recent peat deposits which have not undergone thermal maturation could result from the direct input of αβ hopanoids by indigenous bacteria (Rosa-Putra et al., 2001). Alternatively, it could derive from oxidation and decarboxylation reactions of BHPs followed by isomerization at the C-17 position catalysed by the acidic environment (Ries-Kautt and Albrecht, 1989; Pancost et al., 2003). More recently, Huang et al. (2015) have argued that temperature and hydrology exert a control upon the formation of the C_{31} αβ hopane and it remains unclear why the C_{31} αβ hopane is so abundant in some peatlands. Such findings also complicate the application of geohopanoids as palaeoenvironmental proxies (see Pancost et al., 2003; McClymont et al., 2008; Inglis et al., 2015; Huang et al., 2015).

However, due to the small number of peats that have been studied as well as the lack of peatland diversity sampled, the environmental controls regulating geohopanoid distributions in peats remain poorly constrained. Here, we present the first global study of the occurrence, distribution and diagenesis of geohopanoids within peat using samples (n = 395) obtained from new and previously published datasets spanning a wide temperature (−1 to 27 °C) and pH (3–8) range. Based upon this, we explore how the environment regulates hopanoid isomerisation in modern peatlands by comparing hopanoic acid and hopane ββ/(αβ + ββ) ratios to both temperature and pH estimates. We then explore the utility of geohopanoids as palaeoenvironmental indicators in natural archives.

2. METHODS

2.1. Data compilation

Previously published C_{31} hopane ββ/(αβ + ββ) indices were obtained from the Dajiuhu, Zoige, Hani, and Shiwangutian peatlands in China (Huang et al., 2015) (Fig. 1). These are surface samples collected from 0 to 2 cm depth (n = 63). For full details on each site, see Huang et al. (2015). Previously published C_{31} hopane ββ/(αβ + ββ) indices were also obtained from the Butterburn Flow (UK) peat (McClymont et al., 2008). The samples were collected between 50 and 90 cm depth (n = 26). For full details on this site, see McClymont et al. (2008).

We also present unpublished C_{31} hopane ββ/(αβ + ββ) indices from Butterburn Flow (n = 34; UK; Pancost et al., 2011), Bissendorfer Moor (n = 50; Germany; Pancost et al., 2011), Ballyduff Bog (n = 50; Ireland; Pancost et al., 2011), Kontolanrahka Bog (n = 45; Finland; Pancost et al., 2011) and Hongyuan (n = 26; Tibet; Zheng et al., 2014). For each site (excluding Butterburn Flow) samples were obtained between 0 and 100 cm depth. At Butterburn Flow, samples were collected between 0 and 50 cm depth, and complement the dataset from McClymont et al. (2008). The full experimental procedure for each site is described within the supplementary information.

2.2. Sampling

To generate a global database of geohopanoid distributions, we analysed additional samples (n = 111) from 23 wetlands in 9 different countries (Peru, Indonesia, Brazil, USA, Argentina, Spain, Australia, Germany and Sweden; Fig. 1). Samples were obtained from peat cores spanning the upper 100 cm. The samples cover a broad range in mean annual temperature (MAAT) from −1 to 26 °C. The peats are characterised by a wide variety of vegetation, ranging from *Sphagnum*-dominated ombrotrophic peats to *Cyperaceae*-dominated minerotrophic peats.

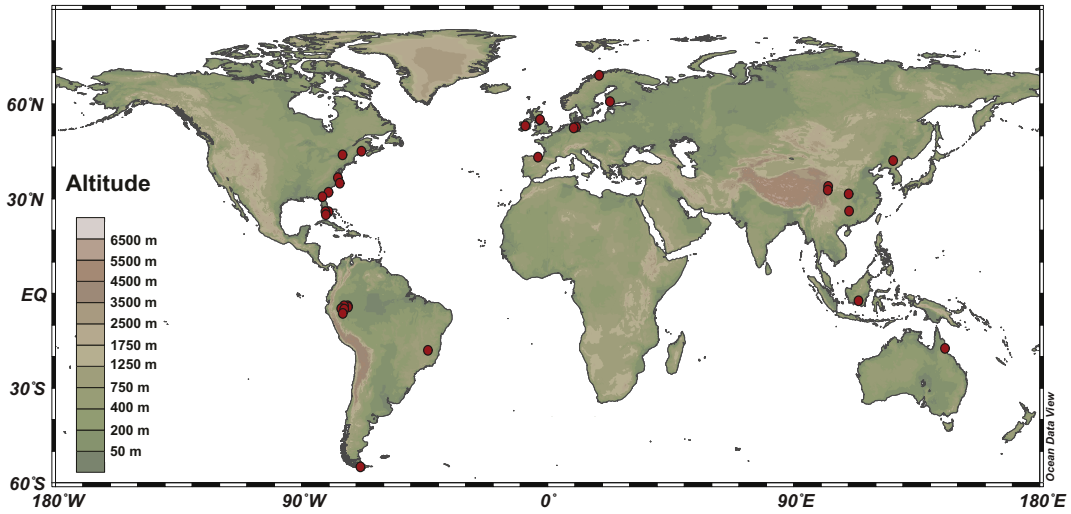

Fig. 1. Map with the location of all peats used in this study. (For interpretation of the references to colour in this figure legend, the reader is referred to the web version of this article.)

2.3. Organic geochemistry

2.3.1. Extraction and separation

Peats (n = 111) were extracted with an Ethos Ex microwave extraction system using 15 ml of dichloromethane (DCM) and methanol (MeOH) (9:1, *v/v*, respectively) at the Organic Geochemistry Unit in Bristol. The microwave program consisted of a 10 min ramp to 70 °C (1000 W), 10 min hold at 70 °C (1000 W), and 20 min cool down. Samples were centrifuged at 1700 rounds per minute for 3–5 min, and the supernatant was removed and collected. A further 10 ml of DCM:MeOH (9:1, *v/v*) was added to the remaining peat material and centrifuged again, after which the supernatant was removed and combined with the previously obtained supernatant. This process was repeated 3–6 times, depending on the volume of sample, to ensure that all extractable lipids were retrieved. The TLE was initially separated over silica into apolar and polar fractions using hexane:dichloromethane (9:1, *v/v*) and dichloromethane:methanol (1:2, *v/v*), respectively. Due to an abundance of aromatic compounds within some apolar fractions, the apolar fractions were subsequently fractionated over silica into saturated hydrocarbon and aliphatic fractions using hexane (100%) and hexane:dichloromethane (3:1, *v/v*) respectively. Note that slightly different methodologies were used by Zheng et al. (2014) and Pancost et al. (2011), as well as for published data from Huang et al. (2015) and McClymont et al. (2008) (see Supplementary Information).

2.3.2. Methylation and silylation

For a subset of samples (35 out of 111), the polar fraction was methylated by adding 100 µl of BF_3/MeOH and heating at 60 °C for 30 min. The sample was cooled down to room temperature before c. 1 ml of DCM-extracted double distilled water was added. This was followed by the addition of ~2 ml of DCM. The fatty acid methyl esters were subsequently extracted from the bottom layer, added to a 7 ml vial, and the process was repeated twice. The sample was dried, redissolved in DCM and eluted through an anhydrous sodium sulphate column to extract any residual water. The column was washed through with DCM three times and the sample dried under N_2 at 40 °C. Prior to analysis, samples were silylated by adding 25 µl of *N,O*-bis(trimethylsilyl)trifluoroacetamide (BSTFA) and 25 µl of pyridine, and heated for one hour at 70 °C. Samples were then allowed to cool and dried down under N_2. Silylated samples were analysed by GC-MS within 24 h.

2.3.3. GC-MS analysis

Samples were analysed using a Thermo Scientific ISQ Single Quadrupole gas chromatography-mass spectrometer (GC-MS). Using helium as the carrier gas, 1 µl of sample (dissolved in ethyl acetate) was injected at 70 °C using an on-column injector. The temperature program included four stages: 70 °C hold for 1 min, 70–130 °C at 20 °C/min rate; 130–300 °C at 4 °C/min; and temperature hold for 20 min at 300 °C. The electron ionisation source was set at 70 eV. Scanning occurred between *m/z* ranges of 50–650 Daltons. The GC was fitted with a fused silica capillary column (50 m × 0.32 mm i.d.) coated with a ZB1 stationary phase (dimethylpolysiloxane equivalent, 0.12 µm film thickness). Geohopanoids (see Fig. A1) were identified based upon published spectra, characteristic mass fragments and retention times (e.g. Uemura and Ishiwatari, 1995; Rohmer et al., 1984; Sessions et al., 2013; Van Dorsselaer et al., 1974).

2.3.4. GC-C-IRMS analysis

GC-MS analysis revealed the occurrence of two unknown C_{30} hopenes (see Sections 3.1 and 4.1 and supplementary information). To assess their potential origin, 15 hydrocarbon fractions from Bissendorfer Moor (Germany) were selected for compound specific stable carbon isotope ($\delta^{13}C$) analysis. These samples span the upper 100 cm and capture both the oxic acrotelm and anoxic catotelm. Gas

chromatography-combustion-isotope ratio mass spectrometry (GC-C-IRMS) was performed using an Isoprime 100 GC-combustion-isotope ratio mass spectrometer system. Samples were measured in duplicate and $\delta^{13}C$ values were converted to VPDB by bracketing with an in-house gas (CO_2) of known $\delta^{13}C$ value. Instrument stability was monitored by regular analysis of an in-house standard. Injection volume was 1 µl onto to a Zebron-I nonpolar column (50 m × 0.32 mm i.d., 0.10 µm film thickness). GC conditions were the same as described above for GC-MS analysis (see Section 2.3.3).

2.4. Environmental parameters

For each site, mean annual air temperature (MAAT) was calculated using the simple bioclimatic model PeatStash, which computes MAAT globally with a 0.5° spatial resolution (Gallego-Sala and Prentice, 2013; Naafs et al., 2017). PeatStash is preferred over (short-term) data from local weather stations as the spatial and temporal coverage of weather stations varies greatly across the globe. Published pH data were used as reported (see Charman et al., 2007; Zheng et al., 2014; Huang et al., 2015). For new sites, pH data were obtained from the literature or during sampling (Naafs et al., 2017).

2.5. Statistical analysis

To assess the role of environmental change upon hopanoid isomerisation ratios, we calculated Deming regressions using the R software package (http://www.R-project.org/). Deming regressions differ from simple linear regressions as they take into account the error on both the *x*- (e.g., proxy) and *y*-axis (e.g., environmental variable) (Adcock, 1878). Here, we assume that the error associated with proxy measurements and environmental parameters is independent and normally distributed. To calculate a Deming regression, we must define the standard deviation (σ) for both the *x*- and *y*-axis. For MAAT, the standard deviation is defined as 1.5 °C (see Naafs et al., 2017). For pH, the standard deviation is defined as 0.5 pH units (see Naafs et al., 2017). For the C_{32} hopanoic acid and C_{31} hopane ββ/(αβ + ββ) indices, the standard deviation and ratio of variance must also be defined (see Supplementary Information). Residuals were calculated for the full dataset using the following equation:

$$Residual_y = y_{observed} - y_{predicted}$$

The root mean square error (RMSE) for *y*, was calculated using the following equation:

$$RSME_y = \sqrt{\frac{\sum_{x=1}^{n}\left(y_{x,observed} - y_{x,predicted}\right)^2}{n}} \times \frac{n}{df}$$

where *df* stands for degrees of freedom, which in this case is n − 1.

To assess the interdependence of temperature and pH upon hopane isomerisation ratios, we also constructed x-y plots of temperature and pH and plotted C_{31} ββ/(αβ + ββ) ratios as a third continuous variable (Fig. A2).

3. RESULTS

3.1. Geohopanoid distributions

In our global dataset, most samples come from strongly acidic peats with pH < 5 (n = 278 samples from 22 settings); however, the data set includes peats from moderately acidic (pH 5–7) and neutral-to-slightly alkaline (pH > 7) peatlands (78 samples from 13 settings and 22 samples from 4 settings, respectively). Within the global dataset, the hydrocarbon fraction contained a range of C_{27}–C_{32} hopanes and C_{27}–C_{30} hopenes (Fig. 2a). Hopanes and/or hopenes were detected in 378 out of 395 samples. The dominant hopanoid in the hydrocarbon fraction was typically the (22R)-17α,21β(H)-homohopane (C_{31}) (Fig. 2a). However, in some settings 17β(H)-trisnorhopane (C_{27}), hop-22 (29)-ene (C_{30}; diploptene) or two C_{30} hopenes with unknown structures dominated the hydrocarbon fraction. The latter are characterised by a molecular ion of *m/z* 410 with a base peak of *m/z* 191, major ions at *m/z* 69, 81, 95, 189 and minor ions at *m/z* 395 (Fig. A3). The hydrocarbon fraction was also characterised by a range of minor compounds, including: 17,21-epoxyhopane, 17α(H)- and 17β(H)-trisnorhopane (C_{27}), 17α,21β(H)- and 17β,21β(H)-norhopane (C_{29}), 17α,21β(H)-, 17 β,21α(H)- and 17β,21β(H)-hopane (C_{30}), (22S)-17α,21β(H)-, (22R)-17β,21α(H)- and -17β,21β(H)-homohopane (C_{31}), 17β,21β(H)-bishomohopane (C_{32}), 22,29,30-Trisnorhop-17(21)-ene (C_{27}), Hop-17(21)-ene (C_{30}) and 2-methylhop-17(21)-ene (C_{31}) (see Figs. 2a and A1).

Within the polar fractions, the dominant compound in most settings was 17β,21β(H)-bishomohopanoic acid (C_{32}) (Fig. 2b). 17α,21β(H)-bishomohopanoic acid (C_{32}) was also relatively abundant. In addition to these major compounds, the polar fraction was characterised by a range of other hopanoids, including: hopan-29-ol (C_{30}; diplopterol), 17β,21β(H)-homohopanoic acid (C_{31}), 17β,21α(H)-bishomohopanoic acid (C_{32}), 17β,21β(H)-bishomohopanol (C_{32}), 17β,21α(H)-trishomohopanoic acid (C_{33}) and 17β,21β(H)-trishomohopanoic acid (C_{33}) (Fig. 2b).

3.2. Geohopanoid isomerisation ratios

The degree of geohopanoid isomerisation was assessed using ββ/(αβ + ββ) and 22S/(22S + 22R) indices (MacKenzie et al., 1980). The global average C_{31} hopane ββ/(αβ + ββ) is relatively low with an average value of 0.23 (n = 378, σ = 0.26; Fig. A4). In contrast, C_{32} hopanoic acid ββ/(αβ + ββ) values were relatively high with an average value of 0.75 (n = 35, σ = 0.19; Fig. A5). In the majority of *Sphagnum* (Fig. 3) and non-*Sphagnum* dominated peatlands (Fig. 4), downcore C_{31} hopane ββ/(αβ + ββ) indices remain stable or slightly decrease with depth. Within a sub-set of our dataset, we also obtained C_{31} 22S/(22S + 22R) indices. As values were low and stable throughout (average = 0.04, n = 106, σ = 0.06), we did not revisit older studies.

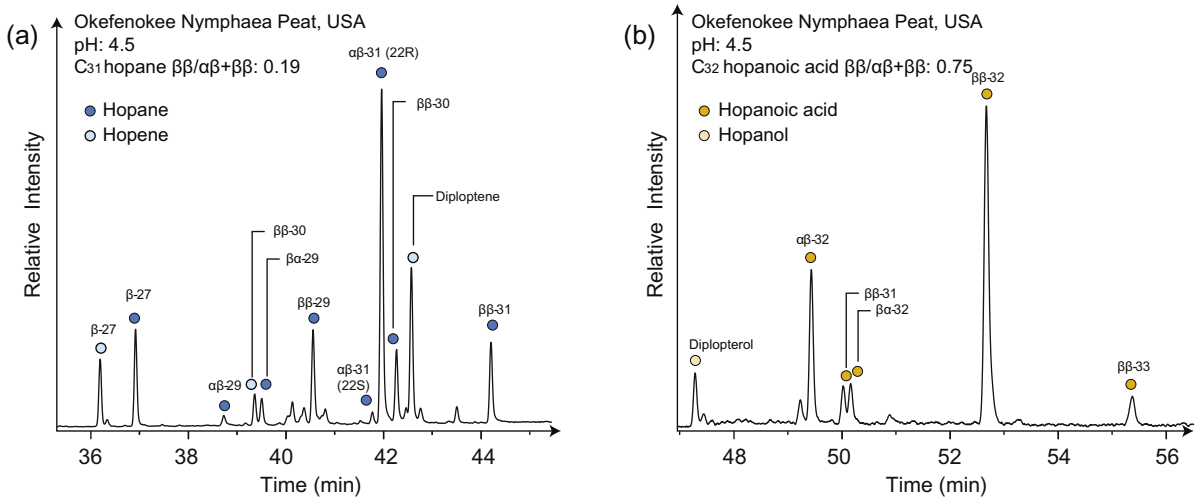

Fig. 2. Partial *m/z* 191 gas chromatogram of a typical (a) hydrocarbon and (b) polar fraction. Numbers accompanied with Greek letters signify the carbon number and stereochemistry of hopanoids.

3.3. Geohopanoid $\delta^{13}C$ values

$\delta^{13}C$ values were determined for 15 samples within Bissendorfer Moor, Germany, where two unknown C_{30} hopenes comprise 30–40% of the hopane/hopene assemblage. The earlier eluting C_{30} hopene $\delta^{13}C$ value ranges from −24.9‰ to −29.9‰ (average: −27.5‰), whereas that of the later eluting C_{30} hopene is more depleted and ranges from −26.5‰ to −34.7‰ (average: −29.7‰). Both values are ^{13}C-depleted (ca. 3–6‰ lower) compared to the C_{31} αβ hopane (average: −24.6 ± 1.0‰) and C_{31} ββ hopane (average: –23.2 ± 1.7‰) for a given sample. For comparison, $\delta^{13}C$ values from higher plant- (C_{29} to C_{33} *n*-alkanes) and eukaryote- (5α-Cholestane) biomarkers in these samples are –33.9 ± 0.3‰ and −25.7 ± 0.1‰, respectively.

4. DISCUSSION

4.1. Geohopanoid distributions in modern peats

Previous studies indicate that peatlands contain a diverse range of geohopanoids (Quirk et al., 1984; Pancost et al., 2003; Zhang et al., 2009; Huang et al., 2015). However, our global dataset indicates that geohopanoid distributions are typically dominated by the C_{32} ββ hopanoic acid (Fig. 2b) and C_{31} αβ hopane (Fig. 2a). This is consistent with previous studies (e.g. Quirk et al., 1984; Ries-Kautt and Albrecht, 1989; Dehmer, 1993; Pancost et al., 2003; Huang et al., 2015; Torres and Pancost, 2016). Also in agreement with previous observations (e.g. Dehmer, 1993; Pancost et al., 2003; Quirk et al., 1984), the C_{31} αβ hopane dominates the hopane

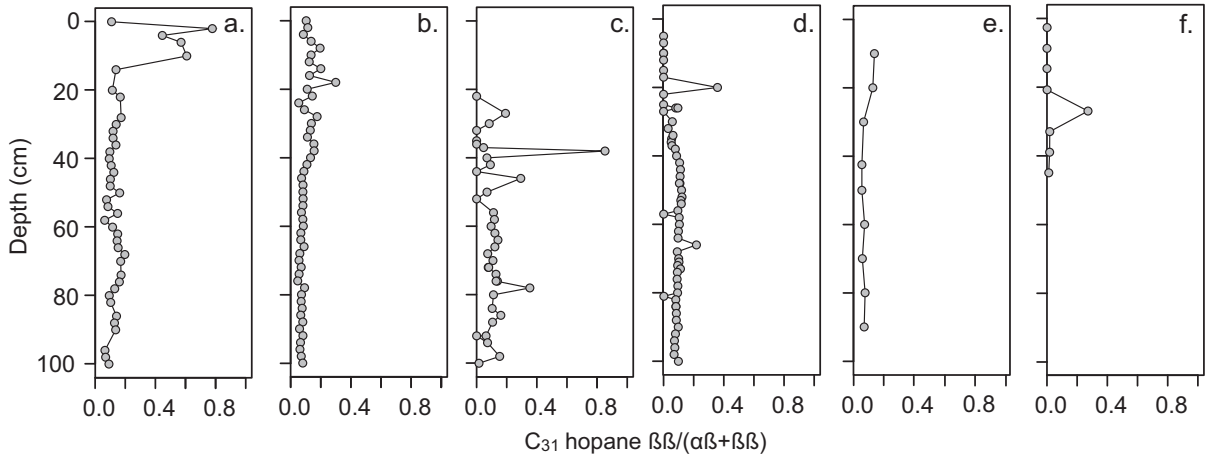

Fig. 3. Downcore C_{31} hopane ββ/αβ + ββ profiles for *Sphagnum*-dominated peatlands. (a) Germany (Bissendorfer Moor), (b) Ireland (Ballyduff Bog), (c) Finland (Kontolanrahka Bog), (d) UK (Butternburn Flow), (e) Germany (Odersprung Bog), (f) Argentina (Tierra del Fuego).

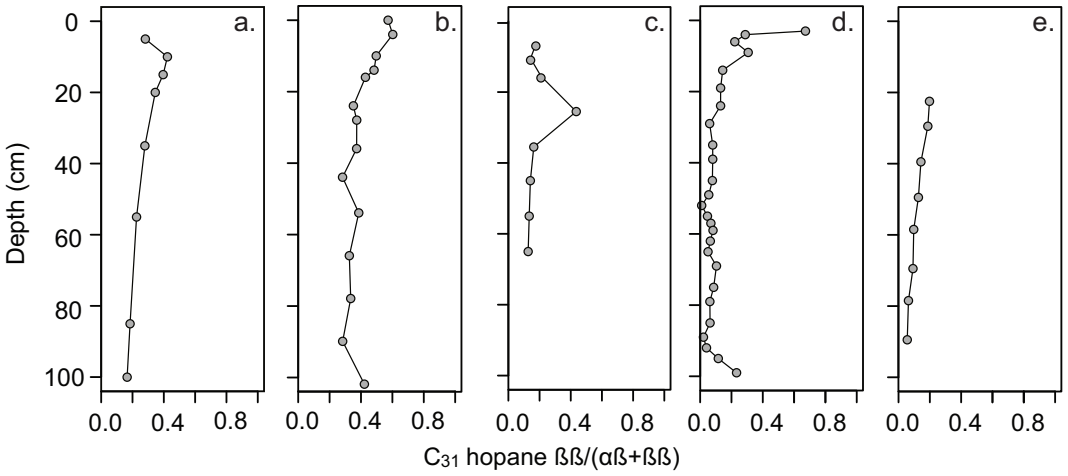

Fig. 4. Downcore C_{31} hopane ββ/αβ + ββ profiles for non-*Sphagnum* peatlands. (a) Indonesia (Sebangau), (b) Brazil (Pinhieros), (c) Spain (Zalama), (d) Tibet (Hongyuan), (e) Australia (Bomfield Swamp).

distribution within acidic (pH < 6), ombrotrophic and *Sphagnum*-dominated peats. In other settings, diploptene is the dominant compound. However, it is found across a wide pH (ca. 3–8) and temperature range (−1 to 26 °C), suggesting it is not restricted in its occurrence (c.f. C_{31} αβ hopane). This is consistent with the fact that diploptene is synthesised by a wide variety of aerobic (Rohmer et al., 1984) and also anaerobic bacteria (Härtner et al., 2005; Sinninghe Damsté et al., 2004).

We also report the occurrence of two unknown C_{30} hopenes within six *Sphagnum*-dominated bogs (see Supplementary Information and Fig. A3). To explore the source of these compounds further, we determined the carbon isotopic composition of these compounds within Bissendorfer Moor (Germany). The C_{30} hopenes are ^{13}C-depleted (ca. 3–6‰) relative to C_{31} hopanes at Bissendorfer Moor and likely derive from bacterial sources consuming a diverse suite of carbon substrates (see Pancost et al., 2003; Inglis et al., 2015). This includes ^{13}C-enriched carbohydrates but also more ^{13}C-depleted organic matter or even methane-derived CO_2. This is consistent with the BHP distribution in Bissendorfer Moor which is dominated by bacteriohopanetetrol, bacteriohopanetetrol cyclitol ether and 35-aminobacteriohopane-32,33,34-triol (i.e. saturated tetrafunctionalised BHPs), suggesting a largely heterotrophic bacterial community with only some evidence for aerobic methanotrophy (Talbot et al., 2016b).

4.2. Diagenesis of geohopanoids in peats

Our results indicate that peatlands are dominated by a range of geohopanoids including hopanoic acids, hopanols, hopanes and hopenes. These compounds can be directly biosynthesised (i.e. diploptene) or derived from BHPs. Although we have not analysed BHPs here, based on previous work (Talbot et al., 2016b; van Winden et al., 2012; Kim et al., 2011) it is likely that they are also widespread. However, the diagenesis of bio- and geohopanoids remains poorly constrained. Whilst most BHPs can be preserved to significant depth (>400 cm) within peatlands, there can be a significant decrease in the concentration of unsaturated BHPs (e.g. unsaturated BHT-pentose) and "soil-marker BHPs" (e.g. adenosylhopane) below the upper surface layer of a *Sphagnum*-dominated bog. This is likely related to diagenesis under highly acidic conditions (e.g. Talbot et al., 2016a, 2016b).

BHPs also undergo oxidative degradation to form a range of degradation products, including hopanoic acids and hopanols (Bisseret and Rohmer, 1995; Adam et al., 2016; Farrimond et al., 2003; Innes et al., 1997; Quirk et al., 1984). Within peat-forming environments, tetrafunctionalised BHPs are associated with the presence of C_{32} hopanoic acids (Ries-Kautt and Albrecht, 1989; Innes et al., 1997). This suggests that diagenesis is analogous to periodic acid/sodium borohydride treatment (i.e. 1,2-diol cleavage), whereby oxidative cleavage of vicinal diols (**1**) gives access to an intermediate C_{32} hopanoid aldehyde (**9**) before undergoing oxidation to form the C_{32} hopanoic acid (**10**) (Zundel and Rohmer, 1985; Peiseler and Rohmer, 1991; Bisseret and Rohmer, 1995). This model is also consistent with the low abundance of penta- and hexafunctionalised BHPs and C_{31} and C_{30} hopanoic acids in peat (Talbot et al., 2016b; *this paper*). Here, we show for the first time that the dominance of C_{32} hopanoic acids in peat is global, suggesting that tetrafunctionalised BHPs dominate within a range of diverse peat-forming environments. It also suggests that similar diagenetic processes are occurring on a global scale.

Previous studies proposed that decarboxylation of the C_{32} hopanoic and/or dehydration of the C_{32} hopanol then yields the C_{31} hopane (Barton et al., 1980; Bennett and Abbott, 1999). Based upon the high abundance of C_{32} hopanoic acids in peat, we suggest that decarboxylation of the C_{32} hopanoic acid **(10–11)** (rather than dehydration of the C_{32} hopanol) is the primary source of the C_{31} hopane **(16–17)** in peat (Fig. 5). This is consistent with Huang et al. (2015) who have shown a statistically significant correlation ($p < 0.01$) between C_{32} hopanoic acid and C_{31} hopane concentrations within a Chinese peatland.

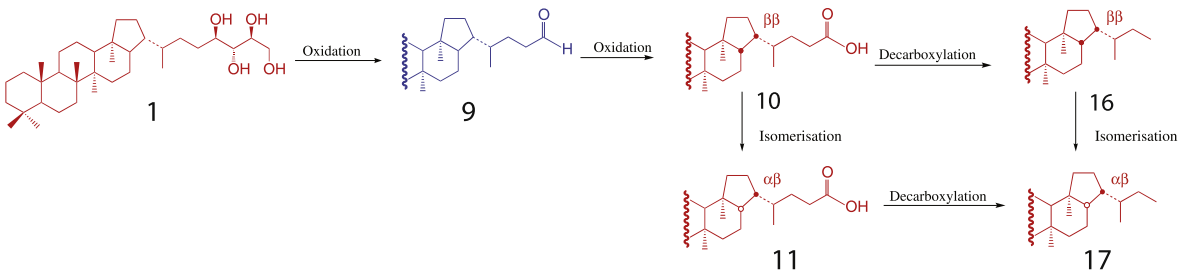

Fig. 5. Proposed steps in the diagenesis of bio- and geohopanoids in peat. The structures in red were identified in modern peats. The structure in blue corresponds to a postulated intermediate. For interpretation of the references to hopanoids in this figure, the reader is referred to the supplementary information. (For interpretation of the references to colour in this figure legend, the reader is referred to the web version of this article.)

Crucially, we show that bio- and geohopanoid diagenesis occurs rapidly in peatlands and geohopanoids are detected within the upper 0–5 cm of many peats. Geohopanoid concentrations usually remain low within the upper oxic layer (<20 cm; Fig. 6), although there are some exceptions (e.g. Kontolanrahka Bog, Finland). Geohopanoid concentrations are substantively higher at the oxic/anoxic boundary (ca. 20–40 cm in our peats; Fig. 6). As hopanoids are predominantly, although not exclusively, derived from aerobic bacteria, this increase is attributed to microbial decomposition and/or transformation of BHPs (Innes et al., 1998; Torres and Pancost, 2016). Below the oxic/anoxic boundary, geohopanoid concentrations are rather variable (Fig. 6), suggesting that additional diagenesis may occur at depth (see also Torres and Pancost, 2016).

Our results also indicate that C_{32} hopanoic acids and C_{32} hopanols occur as αβ- and ββ-stereoisomers in peat, with the ββ-isomer typically dominating (Fig. 2b). In contrast, the C_{31} hopane occurs predominantly as the αβ-stereoisomer (Fig. 2a). An offset between hopanoic acid and hopane isomerisation ratios has been observed in Mesozoic sediments (Bennett and Abbott, 1999; Farrimond et al., 2002), where isomerisation is suppressed for increasingly functionalised compounds (e.g. hopanoic acids and hopanols). Indeed, this may explain the lack of αβ-BHPs in modern peats (Talbot et al., 2016b). We also show that isomerisation occurs rapidly, and αβ hopanes often dominate within the top 5 cm of peatlands (Figs. 3 and 4). This suggests that ββ/(αβ + ββ) ratios in peat are likely set during early diagenesis. However, there can be a

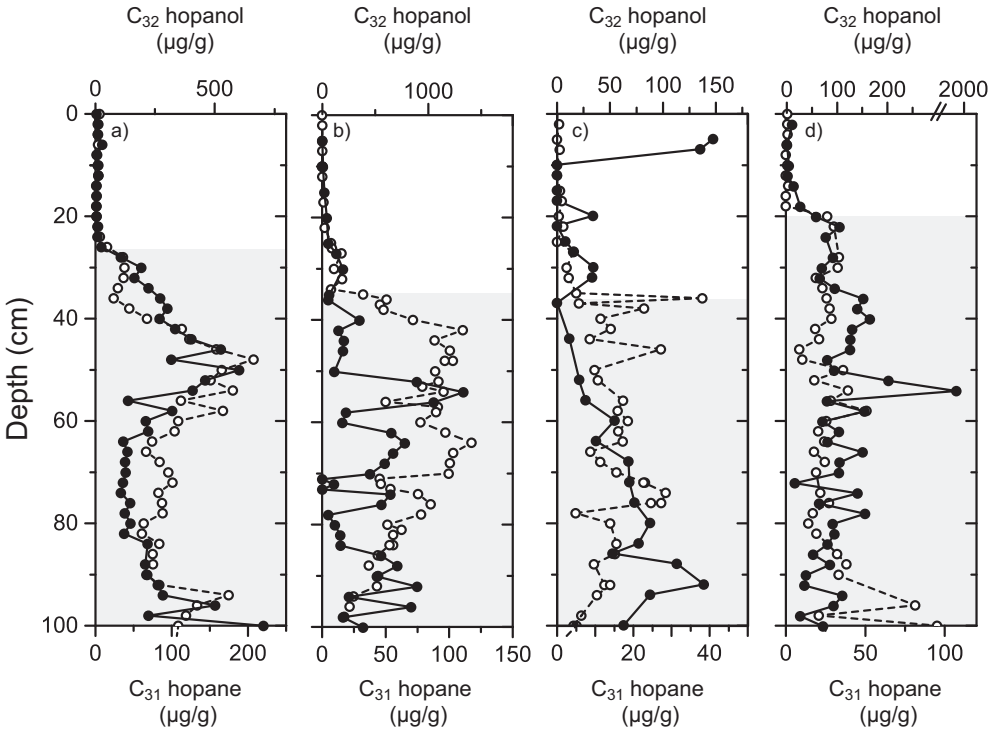

Fig. 6. Geohopanoid abundance with depth. (a) Ballyduff Bog (Ireland), (b) Butterburn Flow (Great Britain), (c) Kontolanrahka Bog (Finland) and (d) Bissendorfer Moor (Germany). Anoxic catotelm denoted in dark grey. Open and closed circles represent hopanes and hopanols, respectively. n.b. the polar fraction was not methylated; as such, hopanoic acids were not GC-amenable under standard conditions and only hopanols were analysed here.

subtle decrease in ββ/(αβ + ββ) ratios with depth (Figs. 3 and 4), suggesting further isomerisation of geohopanoids may occur below the acrotelm/catotelm boundary (see also Section 4.3)

4.3. Environmental controls on geohopanoid isomerisation in peat

Our results indicate that C_{32} hopanoic acids and C_{31} hopanes occur in the αβ-configuration, with a particularly high abundance of the latter. However, it remains unclear why αβ-isomers are so abundant in modern peat. Previous studies have suggested αβ geohopanoids could derive from the direct input of 17α,21β(H)-hopanoids by indigenous bacteria (e.g. Huang et al., 2015). Indeed, Rosa-Putra et al. (2001) reported the presence of 17α,21β(H)- and 17β,21α(H)-biohopanoids alongside the more common ββ isomer in some *Frankia* spp. (Actinobacteria; n.b. the relative abundance of these compounds is unknown). Although Actinobacteria are an important phyla within the peat microbiome (e.g. Dedysh et al., 2006), all biohopanoids observed in modern peatlands occur as a single 17β,21β(H)- isomer (Kim et al., 2011; Talbot et al., 2016b; van Winden et al., 2012). This is true even for early diagenetic intermediate hopanepolyols derived from the degradation of BHPs including: tetrakishomohopane-32,33,34-triol and trishomohopane-32,33-diol (e.g. Rodier et al., 1999; Watson and Farrimond, 2000). The fact that hopanes exhibit a greater degree of isomerisation than functionalised bio- and geohopanoids, their putative precursors, suggests that isomerisation is not inherited from original biological sources. As such, we argue that biosynthesis of αβ-hopanoids is unlikely to directly account for the majority of αβ geohopanoids in peat.

Instead, the occurrence of the C_{31} αβ hopane has been ascribed to acid-catalysed isomerisation (Ries-Kautt and Albrecht, 1989). To explore this further, we compared hopanoic acid and hopane ββ/(αβ + ββ) indices to pH within our global dataset. For sites with only a single pH measurement, we report the average ββ/(αβ + ββ) value (Fig. 7). Both C_{32} hopanoic acid and C_{31} hopane ββ/(αβ + ββ) ratios exhibit a linear positive correlation with pH. The correlation between the C_{31} hopane ββ/(αβ + ββ) index and pH is statistically significant ($r^2 = 0.64$, $p < 0.001$; $n = 94$; Fig. 7a), indicating that pH exerts a first-order control upon hopane isomerisation in peats. In contrast, the correlation between C_{32} hopanoic acid ββ/(αβ + ββ) indices and pH is not statistically significant ($r^2 = 0.13$; $n = 20$; $p = 0.11$ Fig. 7b) and ratios are higher and less variable across the sample set. These features could arise from sedimentary diagenetic constraints. For example, the weak ionic adsorption of functionalised compounds to mineral surfaces could inhibit isomerisation (Farrimond et al., 2002). Farrimond et al. (2002) have also shown that decarboxylation can promote isomerisation through bond cleavage and may explain why the C_{31} hopane isomerisation ratio exhibits a stronger relationship with pH; thus, it might be the decarboxylation step that is crucial to the signal preserved in hopanes.

More recently, Huang et al. (2015) argued that temperature exerts a control upon hopane isomerisation, with enhanced formation of αβ-geohopanoids in warmer settings. However, this conclusion was based upon a single site with a relatively complex evolution history. To explore this further, we compared hopanoic acid and hopane ββ/(αβ + ββ) indices to MAAT within our global dataset. Here, we report the average ββ/(αβ + ββ) value for a given site (Fig. 8; see Supplementary Information). Our results reveal no correlation between C_{31} hopane ββ/(αβ + ββ) indices and MAAT ($r^2 = 0.01$, $p = 0.55$; $n = 35$; Fig. 8b). X-Y plots of temperature and pH with C_{31} ββ/(αβ + ββ) ratios as a third continuous variable support this observation (Fig. A3). Our results also indicate no correlation between C_{32} hopanoic acid ββ/(αβ + ββ) indices and temperature ($r^2 = 0.09$, $p = 0.19$, $n = 20$, Fig. 8a). We attribute this discrepancy to the fact that Huang et al. (2015) utilise a downcore paleo-temperature record, where temperature variations are inferred rather than directly measured.

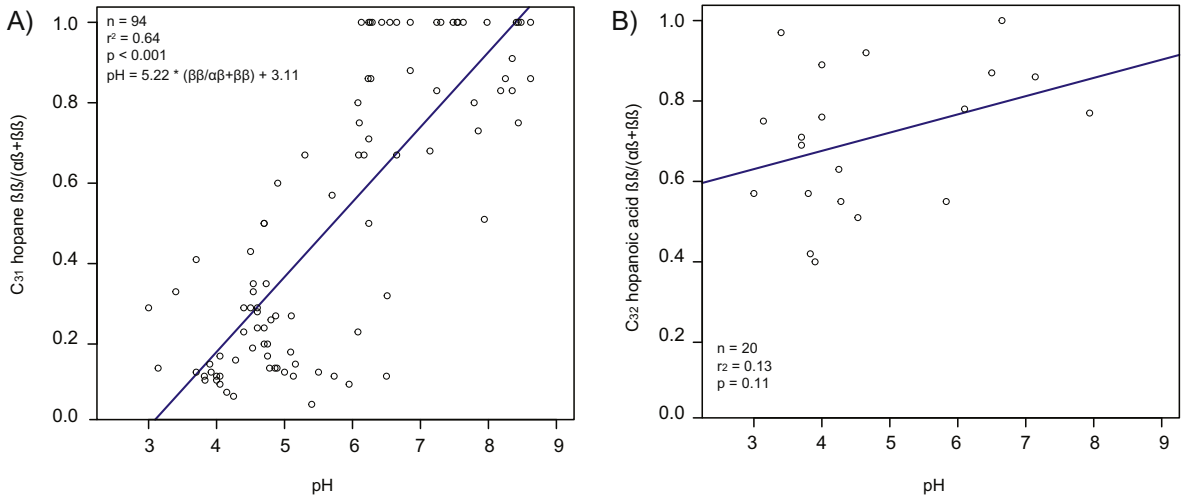

Fig. 7. Impact of pH upon geohopanoid isomerisation. (a) C_{31} hopane ββ/αβ + ββ index vs pH, (b) C_{32} hopanoic acid ββ/αβ + ββ index vs pH.

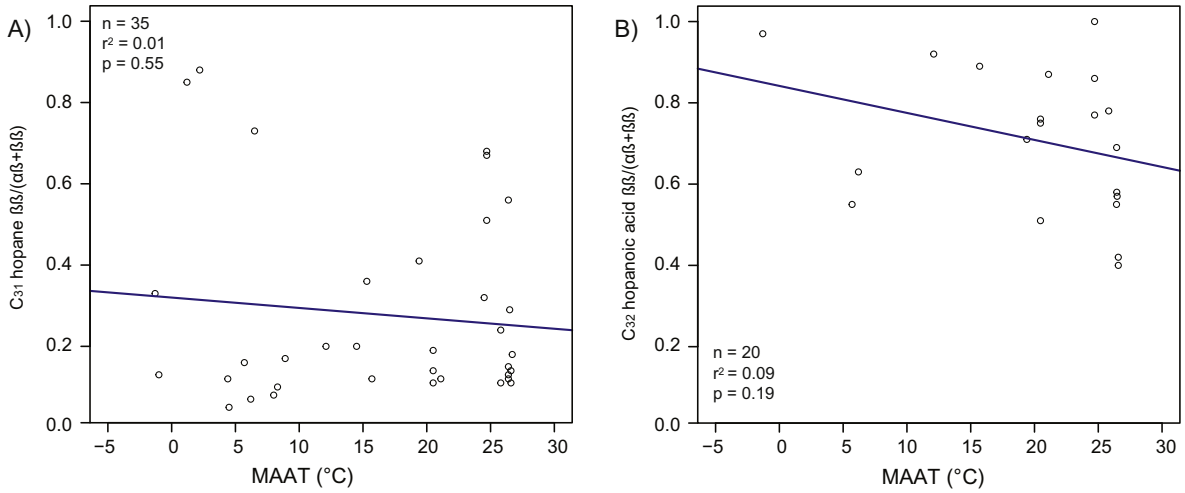

Fig. 8. Impact of temperature upon geohopanoid isomerisation. (a) C_{31} hopane ββ/αβ + ββ index vs MAAT, (b) C_{32} hopanoic acid ββ/αβ + ββ index vs MAAT.

Huang et al. (2015) also argue that hydrological conditions impact geohopanoid isomerisation, with enhanced formation of αβ hopanoids under drier conditions. However, hydrology and pH can be closely linked within peat-forming environments (e.g., Zhong et al., 2017) and extensive rainfall can result in dilution, decreased acidity and a reduction in the formation of αβ-hopanoids (e.g. Pancost et al., 2003). To characterise the impact of hydrology upon hopanoid distributions, future studies should utilise a setting with minor variations in temperature and pH, but large changes in moisture content (c.f. Dang et al. 2016).

There may also be other factors which influence hopanoid isomerisation ratios. For example, Quirk et al. (1984) have argued that vegetation type promotes the formation of αβ hopane. This is based upon an increase in the relative abundance of the C_{31} αβ hopane in a series of *Sphagnum* decay experiments (Quirk, 1984). While this is possible, it does not explain why αβ-hopanoids are rapidly formed in non-*Sphagnum* settings and high acidity seems to be necessary. Likewise, Huang et al. (2015) have suggested that total organic carbon (TOC) content could be important, with enhanced production of αβ-hopanoids in high TOC settings (e.g. Huang et al., 2015). However, this does not explain why ββ-hopanoids dominate in some high TOC settings. Again, high acidity seems to be required.

4.4. Geohopanoids as palaeoenvironmental proxies

Our results support the original hypothesis of Quirk et al. (1984), which suggests that the formation of the αβ hopanoids in peats is strongly dependent on pH. Crucially, isomerisation appears to be fixed during early diagenesis, suggesting that geohopanoid ββ/(αβ + ββ) indices could be a useful proxy for understanding pH over a range of timescales. Here, we utilise the C_{31} hopane ββ/(αβ + ββ) index to construct a peat-specific hopane-based pH proxy:

$$pH = 5.22 * (C_{31}\ \text{hopane}\ \beta\beta/\alpha\beta + \beta\beta) + 3.11\ (n = 94,\ r^2 = 0.64,\ RMSE = 1.4)$$

The coefficient of correlation is stronger than obtained from other peat-specific pH proxies (e.g. the cyclisation of branched glycerol dialkyl glycerol tetraethers (*br*GDGTs); $r^2 = 0.58$, Naafs et al., 2017); however, the RMSE is larger than previously found for *br*GDGTs (see Naafs et al., 2017). Hopane-derived pH estimates were also compared to *br*GDGT-derived pH estimates (CBT_{peat}; Naafs et al., 2017) from the same sample set (Fig. A6). Although the correlation deviates from the 1:1 line - indicating that C_{31} ββ/αβ + ββ ratios give lower pH estimates compared to those obtained using brGDGTs for a given sample - there is a statistically significant correlation between CBT_{peat} and C_{31} ββ/αβ + ββ-based pH values ($p < 0.01$; $r^2 = 0.43$; Fig. A6).

To explore the utility of ββ/(αβ + ββ) indices in natural archives, we calculated downcore pH profiles for each site in our global dataset. All sites exhibit relatively constant pH values within the upper 100 cm and are consistent with relatively stable climate conditions over the last millennium (Crowley, 2000). The only exception is Bissendorfer Moor (Germany), which exhibits a significant decrease in pH (ca. 4 pH units) within the upper 30 cm. However, as the hydrology of this site has been strongly affected by artificial drainage, the surface microbial community may have been affected by human activity (see Talbot et al., 2016b).

It is also possible to calculate pH estimates from previously published datasets. For example, Pancost et al. (2003) observed a subtle increase in ββ/(αβ + ββ) ratios within the Bargerveen peat core during the Sub-Boreal/Sub-Atlantic transition (ca. 2800 years ago; Pancost et al., 2003). This was originally attributed to decreasing acidity (due to enhanced precipitation) and is consistent with our results which indicate a clear pH control on the degree of C_{31} hopane isomerisation. Hopane-derived pH estimates are also relatively low (ca. 3.5) throughout the peat core

and consistent with the abundance of *Sphagnum* moss in the peat (Pancost et al., 2003). However, the magnitude of pH change across the Sub-Boreal/Sub-Atlantic transition is relatively minor (0.2 pH units) and within the error of this proxy. Therefore, we only recommend using ββ/(αβ + ββ) indices to interrogate large amplitude and more long-term pH variation (see below). It is also important to note that the composition of the bacterial community will likely vary between environments (e.g. Lin et al. 2012; Dedysh et al., 2006; Bragina et al., 2012; Serkebaeva et al., 2013). Such changes are likely to impact hopanoid distributions and perhaps isomerisation ratios; however, this is hard to deconvolve and requires further investigation.

The C_{31} ββ/(αβ + ββ) index could also be applied to immature coal deposits (i.e. lignites) to understand environmental change during past greenhouse periods and across hyperthermal events. To explore this, we assessed the geohopanoid distribution within a thermally immature, early Paleogene (~56 Ma) lignite deposit (Schöningen, Germany). Within this setting, the C_{31} αβ isomer dominates the hopane assemblage, suggesting an acidic (pH < 6), ombrotrophic peatland (Fig. 9). This is consistent with the occurrence of *Sphagnum*-type spores and biomarkers within this lignite seam (Inglis et al., 2015; Inglis et al., 2017). Intriguingly, hopane-derived pH values (ca. 4.9) are similar to the average value of 5.0 derived from branched GDGTs (CBT_{peat}; Naafs et al., 2017). Both proxies also exhibit similar temporal trends, although the magnitude of the variations exhibited by the former are larger (Fig. 9).

We have previously suggested that low C_{31} ββ/(αβ + ββ) indices could also be a useful proxy to trace the input of acidic peat (or eroded lignite) to marine or fjord sediments (Inglis et al., 2015; Smittenberg et al., 2004). While our results generally support this hypothesis, some acidic peats exhibit relatively high C_{31} ββ/(αβ + ββ) indices (e.g. Brazil), dictating caution in this approach – in particular, an absence of substantive αβ-hopane inputs should not be interpreted as evidence for an absence of peat inputs. As such, additional lines of evidence should be utilised to trace the input of acidic peat into marine and/or lake sediments (e.g. *Sphagnum* biomarkers and/or *Sphagnum* macrofossils (Nichols and Huang, 2007; McClymont et al., 2011; Nott et al., 2000).

Finally, the ββ/(αβ + ββ) index could also provide insights into pH within other environmental settings. For example, there is a significant correlation between C_{32} hopanoic acid ββ/(αβ + ββ) ratios and pH in a suite of geothermal sinters (pH: from 2.5 to 9.0; $r^2 = 0.85$) (Pancost et al., 2006). However, interpretation of such ratios in older sinters will be more problematic as both temperature and pH, as well as extent of exposure to each of these, will have to be considered.

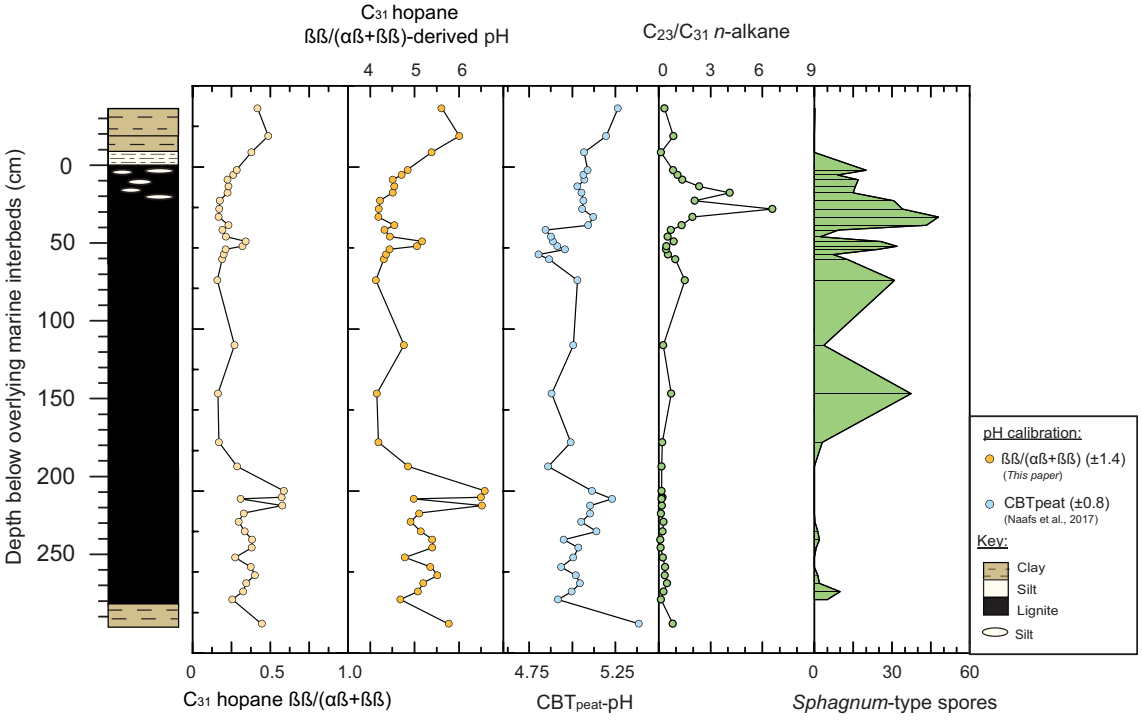

Fig. 9. pH and vegetation change within Seam 1, Schöningen during the latest Paleocene and/or earliest Eocene. (a) the C_{31} hopane ββ/αβ + ββ index, (b) C_{31} hopane ββ/αβ + ββ-derived pH estimates, (c) CBT_{peat}-derived pH estimates (Naafs et al., 2017), (d) C_{23}/C_{31} *n*-alkane ratio (i.e. proxy for input of *Sphagnum* moss; Inglis et al., 2015), (e) the relative abundance (total palynomorphs) of *Sphagnum*-type spores (Inglis et al., 2015). Zero depth marks the top of seam 1 and the base of the overlying marine interbed 2. (For interpretation of the references to colour in this figure legend, the reader is referred to the web version of this article.)

5. CONCLUSIONS

Using >350 samples spanning a wide temperature (−1 to 27 °C) and pH (3–8) range, we have assessed the environmental controls regulating geohopanoid distributions in peats. Our results indicate that peats are characterised by a range of geohopanoids; however, C_{32} hopanoic acids and C_{31} hopanes typically dominate. C_{32} hopanoic acids and C_{31} hopanes both occur in the αβ-configuration and can form almost instantaneously in peatlands (i.e. within the upper 5 cm). This process appears to be strongly regulated by the acidic environment. In particular, the C_{31} hopane isomerisation ratio exhibits a statistically significant correlation with pH. Crucially, there is no correlation between C_{31} hopane isomerisation and temperature. Therefore, our study supports the hypothesis that within peatlands, αβ-hopanoids are acid-catalysed degradation products. This finding suggests that geohopanoid ββ/(αβ + ββ) indices could be used to reconstruct pH within modern and ancient peat-forming environments. Furthermore, we envisage that geohopanoids can provide important new insights into understanding depositional environments and interpreting terrestrial organic matter sources in the geological record.

ACKNOWLEDGEMENTS

This research was funded through the advanced ERC grant 'The Greenhouse Earth System' (T-GRES. Project reference: 340923). RDP acknowledges the Royal Society Wolfson Research Merit Award. YZ thanks the National Natural Science Foundation of China (Project reference: 41372033). ELM acknowledges the Philip Leverhulme Prize. We also thank the NERC Life Sciences Mass Spectrometry Facility (Bristol) for analytical support and D. Atkinson for help with the sample preparation. GNI thanks Janet Dehmer and Philippe Schaeffer for helpful discussions. Members of the T-GRES Peat Database collaborators are M.J. Amesbury, H. Biester, R. Bindler, J. Blewett, M.A. Burrows, D. del Castillo Torres, F.M. Chambers, A.D. Cohen, S.J. Feakins, M. Gałka, A. Gallego-Sala, L. Gandois, D.M. Gray, P.G. Hatcher, E.N. Honorio Coronado, P.D.M. Hughes, A. Huguet, M. Könönen, F. Laggoun-Défarge O. Lähteenoja, M. Lamentowicz, R. Marchant, X. Pontevedra-Pombal, C. Ponton, A. Pourmand, A. M. Rizzuti, L. Rochefort, J. Schellekens, F. De Vleeschouwer. Finally, we thank Darci Rush, Phil Meyers and an anonymous reviewer for their comments and thoughtful suggestions which greatly improved this manuscript.

APPENDIX A. SUPPLEMENTARY MATERIAL

Supplementary data associated with this article can be found, in the online version, at https://doi.org/10.1016/j.gca.2017.12.029.

REFERENCES

Adam P., Schaeffer P., Schmitt G., Bailly L., Courel B., Fresnais M., Fossurier C. and Rohmer M. (2016) Identification and mode of formation of hopanoid nitriles in archaeological soils. *Org. Geochem.* **91**, 100–108.

Barton D. H., Dowlatshahi H. A., Motherwell W. B. and Villemin D. (1980) A new radical decarboxylation reaction for the conversion of carboxylic acids into hydrocarbons. *J. Chem. Soc., Chem. Commun.*, 732–733.

Bennett B. and Abbott G. D. (1999) A natural pyrolysis experiment — hopanes from hopanoic acids? *Org. Geochem.* **30**, 1509–1516.

Birgel D., Thiel V., Hinrichs K.-U., Elvert M., Campbell K. A., Reitner J., Farmer J. D. and Peckmann J. (2006) Lipid biomarker patterns of methane-seep microbialites from the Mesozoic convergent margin of California. *Org. Geochem.* **37**, 1289–1302.

Bisseret P. and Rohmer M. (1995) From bio- to geohopanoids: an efficient abiotic passage promoted by oxygen in the presence of cuprous chloride. *Tetrahedron Lett.* **36**, 7077–7080.

Bradley A. S., Pearson A., Sáenz J. P. and Marx C. J. (2010) Adenosylhopane: the first intermediate in hopanoid side chain biosynthesis. *Org. Geochem.* **41**, 1075–1081.

Bragina A., Berg C., Cardinale M., Shcherbakov A., Chebotar V. and Berg G. (2012) Sphagnum mosses harbour highly specific bacterial diversity during their whole lifecycle. *ISME J.* **6**, 802–813.

Charman D. J. and Blundell A.ACCROTELM members (2007) A new European testate amoebae transfer function for palaeohydrolgical reconstruction on ombrotrophic peatlands. *J. Quat. Sci.* **22**, 209–221.

Crowley T. J. (2000) Causes of climate change over the past 1000 years. *Science* **289**, 270–277.

Dang X., Yang H., Naafs B. D. A., Pancost R. D. and Xie S. (2016) Evidence of moisture control on the methylation of branched glycerol dialkyl glycerol tetraethers in semi-arid and arid soils. *Geochim. Cosmochim. Acta* **189**, 24–36.

Dedysh S. N., Pankratov T. A., Belova S. E., Kulichevskaya I. S. and Liesack W. (2006) Phylogenetic analysis and in situ identification of bacteria community composition in an acidic sphagnum peat bog. *Appl. Environ. Microbiol.* **72**, 2110–2117.

Dehmer J. (1993) Petrology and organic geochemistry of peat samples from a raised bog in Kalimantan (Borneo). *Org. Geochem.* **20**, 349–362.

Farrimond P., Griffiths T. and Evdokiadis E. (2002) Hopanoic acids in Mesozoic sedimentary rocks: their origin and relationship with hopanes. *Org. Geochem.* **33**, 965–977.

Farrimond P., Love G. D., Bishop A. N., Innes H. E., Watson D. F. and Snape C. E. (2003) Evidence for the rapid incorporation of hopanoids into kerogen. *Geochim. Cosmochim. Acta* **67**, 1383–1394.

Farrimond P., Taylor A. and TelnÆs N. (1998) Biomarker maturity parameters: the role of generation and thermal degradation. *Org. Geochem.* **29**, 1181–1197.

Gallego-Sala A. V. and Prentice I. C. (2013) Blanket peat biome endangered by climate change. *Nat. Clim. Change* **3**, 152–155.

Handley L., Talbot H. M., Cooke M. P., Andersoon K. E. and Wagner T. (2010) Bacteriohopanepolyols as tracers for continental and marine organic matter supply and phases of enhanced nitrogen cycling on the late Quaternary Congo deep sea fan. *Org. Geochem.* **41**, 910–914.

Härtner T., Straub K. L. and Kannenberg E. (2005) Occurrence of hopanoid lipids in anaerobic Geobacter species. *FEMS Microbiol. Lett.* **243**, 59–64.

Höfle S. T., Kusch S., Talbot H. M., Mollenhauer G., Zubrzycki S., Burghardt S. and Rethemeyer J. (2015) Characterisation of bacterial populations in Arctic permafrost soils using bacteriohopanepolyols. *Org. Geochem.* **88**, 1–16.

Huang X., Meyers P. A., Xue K., Gong L., Wang X. and Xie S. (2015) Environmental factors affecting the low temperature

isomerization of homohopanes in acidic peat deposits. *Geochim. Cosmochim. Acta.* **154**, 212–228.

Inglis G. N., Collinson M. E., Riegel W., Wilde V., Robson B. E., Lenz O. K. and Pancost R. D. (2015) Ecological and biogeochemical change in an early Paleogene peat-forming environment: linking biomarkers and palynology. *Palaeogeogr. Palaeoclimatol. Palaeoecol.* **438**, 245–255.

Inglis G. N., Collinson M. E., Riegel W., Wilde V., Farnsworth A., Lunt D. J., Valdes P., Robson B. E., Scott A. C., Lenz O. K., Naafs B. D. A. and Pancost R. D. (2017) Mid-latitude continental temperatures through the early Eocene in western Europe. *Earth Planet. Sci. Lett.* **460**, 86–96.

Innes H. E., Bishop A. N., Fox P. A., Head I. M. and Farrimond P. (1998) Early diagenesis of bacteriohopanoids in recent sediments of Lake Pollen, Norway. *Org. Geochem.* **29**, 1285–1295.

Innes H. E., Bishop A. N., Head I. M. and Farrimond P. (1997) Preservation and diagenesis of hopanoids in recent lacustrine sediments of Priest Pot, England. *Org. Geochem.* **26**, 565–576.

Kannenberg E. L. and Poralla K. (1999) Hopanoid biosynthesis and function in bacteria. *Naturwissenschaften* **86**, 168–176.

Kim J. H., Talbot H. M., Zarzycka B., Bauersachs T. and Wagner T. (2011) Occurrence and abundance of soil-specific bacterial membrane lipid markers in the Têt watershed (southern France): soil-specific BHPs and branched GDGTs. *Geochem. Geoph. Geosy.* **12**.

Lin X., Green S., Tfaily M. M., Prakash O., Konstantinidis K. T., Corbett J. E., Chanton J. O., Cooper W. T. and Kostka J. E. (2012) Microbial community structure and activity linked to contrasting biogeochemical gradients in bog and fen environments of the glacial lake Agassiz Peatland. *Appl. Environ. Microbiol.* **78**, 7023–7031.

Mackenzie A., Patience R., Maxwell J., Vandenbroucke M. and Durand B. (1980) Molecular parameters of maturation in the Toarcian shales, Paris Basin, France—I. Changes in the configurations of acyclic isoprenoid alkanes, steranes and triterpanes. *Geochim. Cosmochim. Acta* **44**, 1709–1721.

McClymont E. L., Bingham E. M., Nott C. J., Chambers F. M., Pancost R. D. and Evershed R. P. (2011) Pyrolysis GC–MS as a rapid screening tool for determination of peat-forming plant composition in cores from ombrotrophic peat. *Org. Geochem.* **42**, 1420–1435.

McClymont E. L., Mauquoy D., Yeloff D., Broekens P., van Geel B., Charman D. J., Pancost R. D., Chambers F. M. and Evershed R. P. (2008) The disappearance of Sphagnum imbricatum from Butterburn Flow, UK. *Holocene* **18**, 991–1002.

Naafs B. D. A., Inglis G. N., Zheng Y., Amesbury M. J., Biester H., Bindler R., Blewett J., Burrows M. A., del Castillo Torres D., Chambers F. M., Cohen A. D., Evershed R. P., Feakins S. J., Gałka M., Gallego-Sala A., Gandois L., Gray D. M., Hatcher P. G., Honorio Coronado E. N., Hughes P. D. M., Huguet A., Könönen M., Laggoun-Défarge F., Lähteenoja O., Lamentowicz M., Marchant R., McClymont E., Pontevedra-Pombal X., Ponton C., Pourmand A., Rizzuti A. M., Rochefort L., Schellekens J., De Vleeschouwer F. and Pancost R. D. (2017) Introducing global peat-specific temperature and pH calibrations based on brGDGT bacterial lipids. *Geochim. Cosmochim. Acta* **208**, 285–301.

Nichols J. E. and Huang Y. (2007) C23–C31 n-alkan-2-ones are biomarkers for the genus Sphagnum in freshwater peatlands. *Org. Geochem.* **38**, 1972–1976.

Nott C. J., Xie S., Avsejs L. A., Maddy D., Chambers F. M. and Evershed R. P. (2000) N-Alkane distributions in ombrotrophic mires as indicators of vegetation change related to climatic variation. *Org. Geochem.* **31**, 231–235.

Pancost R., Pressley S., Coleman J., Talbot H., Kelly S., Farrimond P., Schouten S., Benning L. and Mountain B. (2006) Composition and implications of diverse lipids in New Zealand geothermal sinters. *Geobiology* **4**, 71–92.

Pancost R. D., Baas M., van Geel B. and Sinninghe Damsté J. S. (2003) Response of an ombrotrophic bog to a regional climate event revealed by macrofossil, molecular and carbon isotopic data. *Holocene* **13**, 921–932.

Pancost R. D., McClymont E. L., Bingham E. M., Roberts Z., Charman D. J., Hornibrook E. R. C., Blundell A., Chambers F. M. , Lim K. L. H. and Evershed R. P. (2011) Archaeol as a methanogen biomarker in ombrotrophic bogs. *Org. Geochem.* **42**, 1279–1287.

Pancost R. D., Steart D. S., Handley L., Collinson M. E., Hooker J. J., Scott A. C., Grassineau N. V. and Glasspool I. J. (2007) Increased terrestrial methane cycling at the Palaeocene-Eocene thermal maximum. *Nature* **449**, 332–335.

Pearson A., Flood Page S. R., Jorgenson T. L., Fischer W. W. and Higgins M. B. (2007) Novel hopanoid cyclases from the environment. *Environ. Microbiol.* **9**, 2175–2188.

Peiseler B. and Rohmer M. (1991) Prokaryotic triterpenoids. (22R,32R)-34,35-Dinorbacteriohopane-32,33-diols from Acetobacter aceti ssp. xylinum: new bacteriohopane derivatives with shortened side-chain. *J. Chem. Soc.*, 2449–2453.

Peters K. and Moldowan J. (1991) Effects of source, thermal maturity, and biodegradation on the distribution and isomerization of homohopanes in petroleum. *Org. Geochem.* **17**, 47–61.

Quirk M., Wardroper A., Wheatley R. and Maxwell J. (1984) Extended hopanoids in peat environments. *Chem. Geol.* **42**, 25–43.

Ries-Kautt M. and Albrecht P. (1989) Hopane-derived triterpenoids in soils. *Chem. Geol.* **76**, 143–151.

Rodier C., Llopiz P. and Neunlist S. (1999) C_{32} and C_{34} hopanoids in recent sediments of European lakes: novel intermediates in the early diagenesis of biohopanoids. *Org. Geochem.* **30**, 713–716.

Rohmer M., Bouvier-Nave P. and Ourisson G. (1984) Distribution of hopanoid triterpenes in prokaryotes. *Microbiol.* **130**, 1137–1150.

Rosa-Putra S., Nalin R., Domenach A.-M. and Rohmer M. (2001) Novel hopanoids from Frankia spp. and related soil bacteria. *Eur. J. Biochem.* **268**, 4300–4306.

Sáenz J. P., Grosser D., Bradley A. S., Lagny T. J., Lavrynenko O., Broda M. and Simons K. (2015) Hopanoids as functional analogues of cholesterol in bacterial membranes. *PNAS* **112**, 11971–11976.

Schefuß E., Eglinton T. I., Spencer-Jones C. L., Rullkötter J., De Pol-Holz R., Talbot H. M., Grootes P. M. and Schneider R. R. (2016) Hydrologic control of carbon cycling and aged carbon discharge in the Congo River basin. *Nat. Geosci.* **9**, 687.

Seifert W. K. and Moldowan J. M. (1980) The effect of thermal stress on source-rock quality as measured by hopane stereochemistry. *Phys. Chem. Earth* **12**, 229–237.

Serkebaeva Y. M., Kim Y., Liesack W. and Dedysh S. N. (2013) Pyrosequencing-based assessment of the bacteria diversity in surface and subsurface peat layers of a norther wetland, with focus on poorly studies phyla and candidate divisions. *PLoS ONE* **8**, e63994.

Sessions A. L., Zhang L., Welander P. V., Doughty D., Summons R. E. and Newman D. K. (2013) Identification and quantification of polyfunctionalized hopanoids by high temperature gas chromatography–mass spectrometry. *Org. Geochem.* **56**, 120–130.

Sinninghe Damsté J. S., Rijpstra W. I. C., Schouten S., Fuerst J. A., Jetten M. S. and Strous M. (2004) The occurrence of

hopanoids in planctomycetes: implications for the sedimentary biomarker record. *Org. Geochem.* **35**, 561–566.

Smittenberg R., Pancost R., Hopmans E., Paetzel M. and Damsté J. S. (2004) A 400-year record of environmental change in an euxinic fjord as revealed by the sedimentary biomarker record. *Palaeogeogr. Palaeoclimatol. Palaeoecol.* **202**, 331–351.

Spencer-Jones C. L., Wagner T. and Talbot H. M. (2017) A record of aerobic methane oxidation in tropical Africa over the past 2.5 Ma. *Geochim. Cosmochim. Acta* **218**, 27–39.

Talbot H. M., Bischoff J., Inglis G. N., Collinson M. E. and Pancost R. D. (2016a) Polyfunctionalised bio- and geohopanoids in the Eocene Cobham Lignite. *Org. Geochem.* **96**, 77–92.

Talbot H. M. and Farrimond P. (2007) Bacterial populations recorded in diverse sedimentary biohopanoid distributions. *Org. Geochem.* **38**, 1212–1225.

Talbot H. M., Handley L., Spencer-Jones C. L., Dinga B. J., Schefuß E., Mann P. J., Poulsen J. R., Spencer R. G., Wabakanghanzi J. N. and Wagner T. (2014) Variability in aerobic methane oxidation over the past 1.2 Myrs recorded in microbial biomarker signatures from Congo fan sediments. *Geochim. Cosmochim. Acta* **133**, 387–401.

Talbot H. M., McClymont E. L., Inglis G. N., Evershed R. P. and Pancost R. D. (2016b) Origin and preservation of bacteriohopanepolyol signatures in Sphagnum peat from Bissendorfer Moor (Germany). *Org. Geochem.* **97**, 95–110.

Torres L. C. and Pancost R. D. (2016) Insoluble prokaryotic membrane lipids in a Sphagnum peat: Implications for organic matter preservation. *Org. Geochem.* **93**, 77–91.

Uemura H. and Ishiwatari R. (1995) Identification of unusual 17β (H)-moret-22 (29)-ene in lake sediments. *Org. Geochem.* **23**, 675–680.

Van Dorsselaer A., Ensminger A., Spyckerelle C., Dastillung M., Sieskind O., Arpino P., Albrecht P., Ourisson G., Brooks P. and Gaskell S. (1974) Degraded and extended hopane derivatives (C 27 to C 35) as ubiquitous geochemical markers. *Tetrahedron Lett.* **15**, 1349–1352.

van Winden J. F., Talbot H. M., De Vleeschouwer F., Reichart G.-J. and Sinninghe Damsté J. S. (2012) Variation in methanotroph-related proxies in peat deposits from Misten Bog, Hautes-Fagnes, Belgium. *Org. Geochem.* **53**, 73–79.

Watson D. F. and Farrimond P. (2000) Novel polyfunctionalised geohopanoids in a recent lacustrine sediment (Priest Pot, UK). *Org. Geochem.* **31**, 1247–1252.

Zhang Z., Wang C., Qiu X., Huang X. and Xie S. (2009) Occurrence of highly abundant bacterial hopanoids in Dajiuhu peatland, central China. *Front. Earth. Sci. China* **3**, 320–326.

Zheng Y., Singarayer J. S., Cheng P., Yu X., Liu Z., Valdes P. J. and Pancost R. D. (2014) Holocene variations in peatland methane cycling associated with the Asian summer monsoon system. *Nat. Comms.* **5**, 4631.

Zhong Q., Chen H., Liu L., He Y., Zhu D., Jiang L., Zhan W. and Hu J. (2017) Water table drawdown shapes the depth-dependant variations in prokaryotic diversity and structure in Zoige peatlands. *FEMS Micro. Eco.* **93**, fix049.

Zundel M. and Rohmer M. (1985) Prokaryotic triterpenoids. *FEBS* **150**, 23–27.

Associate Editor: Elizabeth Ann Canuel